DALTON

Crystal structure, luminescence and other properties of some lanthanide complexes of the polypyridine ligand 6,6′-bis[bis(2-pyridylmethyl)aminomethyl]-2,2′-bipyridine

Anders Døssing,*[a] Hans Toftlund,[b] Alan Hazell,[c] James Bourassa[d] and Peter C. Ford[d]

[a] *Department of Chemistry, University of Copenhagen, Universitetsparken 5, DK-2100 Copenhagen Ø, Denmark*
[b] *Department of Chemistry, Odense University, DK-5230 Odense M, Denmark*
[c] *Department of Chemistry, Aarhus University, DK-8000 Århus C, Denmark*
[d] *Department of Chemistry, University of California, Santa Barbara, CA 93106, USA*

Europium(III) and gadolinium(III) form 1 : 1 complexes with the octadentate polypyridine ligand 6,6′-bis[bis(2-pyridylmethyl)aminomethyl]-2,2′-bipyridine L^2. The crystal structure of the complex $[GdL^2Cl_2]Cl\cdot 2H_2O\cdot 0.5EtOH$ has been determined. The gadolinium atom is co-ordinated to seven nitrogen atoms of the L^2 ligand and two chloride ligands. One of the pyridine groups of L^2 is dangling unco-ordinated. Irradiation of water or MeOH solutions of the $[EuL^2]Cl_3$ complex with UV light led to a metal-centred luminescence. The luminescence lifetimes at 296 K in water, D_2O, MeOH and CD_3OD were 0.78, 1.28, 0.98 and 1.25 ms, respectively. From these data the average number of co-ordinated solvent molecules (water or MeOH) was calculated to be 0.5 according to earlier empirical correlations. The luminescence consists of a series of narrow lines corresponding to the envelopes of $^5D_0 \longrightarrow {}^7F_J$ transitions, the most intense occurring at 613 nm ($\rightarrow {}^7F_2$). The integrated intensities of these emission lines give the respective quantum yields of 0.046 and 0.089 in water and D_2O. The equilibrium constant for formation of the europium complex in MeOH, $I = 0.100$ mol dm^{-3} NBu_4ClO_4, was determined to be $10^{7.09 \pm 0.09}$ dm^3 mol^{-1}.

Recent years have witnessed considerable interest in the preparation and characterization of new materials based on the luminophores europium(III) and terbium(III) that display luminescence in aqueous solution.[1] Such europium(III) or terbium(III) complexes are luminescent in aqueous solution if three conditions are fulfilled: (*i*) the ligand includes a highly absorbing chromophore (since the f–f transitions in the metal have very low molar absorption coefficients), (*ii*) energy transfer from the ligand-centred excited states to the metal centre is fast and efficient, (*iii*) water is largely excluded from the first co-ordination sphere, since the non-radiative deactivation pathway for the excited metal atom is promoted by the high-frequency vibrational modes of H_2O. The antenna effect represented by a combination of requirements (*i*) and (*ii*)[2] makes the ligand design crucial to the photophysical properties of the complexes. Branched macrocyclic ligands containing bipyridine or phenanthroline chromophores have proved especially useful in this regard. Among the first systems to be investigated in this context were the europium(III) and terbium(III) complexes of the cage ligand L^1.[1a,1b] Comparisons of the luminescence lifetimes in water and D_2O solutions using the empirical correlation described below suggested that in aqueous solutions the complexes $[EuL^1]^{3+}$ and $[TbL^1]^{3+}$ each had an average of two to three water molecules present in the first co-ordination spheres. A later crystal structure determination confirmed that (in the solid) two water molecules were indeed co-ordinated.[3]

The present investigation describes the preparation and characterization of gadolinium(III) and europium(III) complexes of the potentially octadentate ligand 6,6′-bis[bis(2-pyridylmethyl)aminomethyl]-2,2′-bipyridine L^2. Comparison of the drawings of L^1 and L^2 illustrates the structural relationship between the two; L^2 can be imagined to be the result of hydrogenolysis of the 2,2′ C–C bonds in two of the bipyridines of L^1 to give a more flexible podand-type compound.

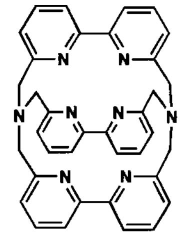

L^1

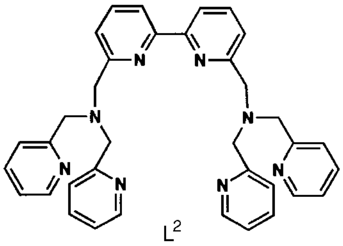

L^2

Experimental

Reagents

The compounds $EuCl_3\cdot 6H_2O$ (99.99%), $GdCl_3\cdot 6H_2O$ and D_2O (99.9%) were obtained from Aldrich. Solvents for spectroscopy were 'spectroscopic grade' and water was doubly distilled. Tetra-*n*-butylammonium perchlorate was obtained from Fluka and dried at 363 K under reduced pressure prior to use.

Preparation

L^2. This compound was prepared as described elsewhere.[4] UV/VIS (MeOH, $I = 0.100$ mol dm^{-3} NBu_4ClO_4): λ_{max}/nm

245, 261, 267 and 288 (10^{-3} ε/dm^3 mol^{-1} cm^{-1} 15.0, 20.0, 19.1 and 16.9).

[EuL^2]Cl$_3$·1.5H$_2$O 1. A mixture of EuCl$_3$·6H$_2$O (195 mg, 0.532 mmol), MeCN (30 cm^3) and trimethyl orthoformate (3.5 cm^3, 32 mmol) was refluxed for 4 h with stirring. Then L^2 (308 mg, 0.532 mmol) was added, and the mixture was refluxed for an additional hour. The solvent was then removed, and the slightly yellow residue dissolved in ethanol (5 cm^3). The solution was filtered, and the complex reprecipitated by addition of diethyl ether (50 cm^3). It was washed with diethyl ether then dried in vacuum (400 mg). The crude product was redissolved in ethanol (3 cm^3), the solution was filtered, and the complex reprecipitated by vapour diffusion of diethyl ether into the ethanol solution. The final step was repeated several times yielding a white product (*ca*. 200 mg) (Found: C, 49.8; H, 4.4; N, 12.8. $C_{36}H_{37}Cl_3EuN_8O_{1.5}$ requires C, 50.0; H, 4.3; N, 13.0%).

[GdL^2]Cl$_3$·5H$_2$O 2. This complex was made as for **1** (Found: C, 46.4; H, 4.3; N, 12.1. $C_{36}H_{44}Cl_3GdN_8O_5$ requires C, 46.6; H, 4.8; N, 12.1%).

Absorption spectra

The UV/VIS absorption spectra were measured on a Perkin-Elmer Lambda 17 spectrophotometer.

Crystallography

X-Ray-quality crystals of [GdL^{2}Cl$_2$]Cl·2H$_2$O·0.5EtOH were obtained by vapour diffusion of diethyl ether into an ethanol solution of complex **2**. A colourless crystal of dimensions 0.45 × 0.50 × 0.58 mm was mounted on a Huber diffractometer and the cell dimensions determined from setting angles of 30 reflections measured at ±2θ with graphite-monochromatized Mo-Kα radiation (λ = 0.710 73 Å). Intensity data were measured at 294 K using ω–2θ scans; two standard reflections were measured every 50. Crystal data are given in Table 1. Intensity data are corrected for background, Lorentz-polarization effects, decay and absorption.[5] The structure was determined by direct methods using SIR 92[6] followed by Fourier-difference syntheses. In the full-matrix least-squares refinement (on *F*) the pyridylmethyl groups were constrained[7] to be identical as were the pyridylmethyl halves of the dimethylbipyridines. Gadolinium and chlorine atoms were refined anisotropically, non-hydrogen atoms isotropically and hydrogen atoms on the ligands were kept at calculated positions with U_{iso} 20% larger than that of the atom to which they were attached. A Rogers factor[8] refined to η = 0.04(10) indicating that the crystal was twinned containing almost equal numbers of domains of opposite polarity. The final *R* and *R′* values were 0.057 and 0.071 for 4945 reflections with $I > 3\sigma(I)$. Atomic scattering factors, f' and f'', were taken from ref. 9.

Atomic coordinates, thermal parameters, and bond lengths and angles have been deposited at the Cambridge Crystallographic Data Centre (CCDC). See Instructions for Authors, *J. Chem. Soc., Dalton Trans.*, 1997, Issue 1. Any request to the CCDC for this material should quote the full literature citation and the reference number 186/316.

Luminescence spectra and lifetimes

For lifetime measurements, solutions of complex **1** were pipetted into Pyrex cells (2 cm diameter) fitted with Rotoflow stopcocks and deaerated by five freeze–pump–thaw cycles. Emission lifetimes were determined as described[10] but with some modifications and updating of the instrumentation. The excitation source was the third harmonic (355 nm) of a Continuum NY-61-20 Q-switched Nd/YAG pulsed laser (operating at 10 Hz with a pulse width of 10 ns). The emission was monitored at right angles to the excitation beam through a SPEX model 1680 Doublemate grating monochromator using an RCA 8852 PMT detector. The PMT output was recorded by an Tektronix TDS 540 digital oscilloscope and transferred to a dedicated Teltron 484 PC work station for data analysis and storage. The 100 digitized waveforms were signal averaged (500 points per waveform) and analysed by single-exponential curve fitting. Emission and excitation spectra were recorded on a SPEX Fluorolog[11] spectrofluorimeter with a water-cooled Hamamatsu R928A PMT corrected for phototube response. For room-temperature luminescence spectra, square Suprasil quartz cells were used for the solutions. For the solid and for the solutions at 77 K, cylindrical 0.5 cm diameter quartz cells were used to obtain emission spectra. Luminescence quantum yields were determined by comparing the integrated emission intensity of the europium(III) complex in solution to that of [Ru(bipy)$_3$]Cl$_2$ (bipy = 2,2′-bipyridine) in water.[12] Typical concentrations of **1** in these experiments were ≈10^{-6} mol dm^{-3}.

Table 1 Crystal data for [GdL^{2}Cl$_2$]Cl·2H$_2$O·0.5EtOH

Formula	$C_{36}H_{34}Cl_3GdN_8 \cdot 2H_2O \cdot 0.5C_2H_6O$
M	901.43
Crystal symmetry	Monoclinic
Space group	$P2_1$
a/ Å	12.652(4)
b/ Å	14.670(7)
c/ Å	20.860(9)
β/°	90.022(23)
U/Å^3	3872(3)
Z	4
D_c/g cm^{-3}	1.546
μ(Mo-Kα)/cm^{-1}	19.73
No. of reflections	7083
No. observed [$I > 3\sigma(I)$], N_o	4945
No. of variables, N_v	304
R^a	0.057
R'^b	0.071
S^c	1.40

[a] $R = \Sigma\left||F_o| - |F_c|\right|/\Sigma|F_o|$. [b] $R' = [\Sigma w(|F_o| - |F_c|)^2/\Sigma w|F_o|^2]^{\frac{1}{2}}$, $w = 1/\{[\sigma(F_o^2) + 1.03F_o^2]^{\frac{1}{2}} - |F_o|\}$ with $\sigma(F_o^2)$ from counting statistics. [c] $S = [\Sigma w(|F_o| - |F_c|)^2/(N_o - N_v)]^{\frac{1}{2}}$.

Results and Discussion

Crystal structure

The asymmetric unit consists of two [GdL^{2}Cl$_2$]$^+$ cations, two chloride ions, four waters of crystallization and a solvent molecule presumed to be ethanol. The gadolinium atoms are co-ordinated to seven nitrogen atoms of the L^2 ligand and two chlorine atoms, and one of the pyridine groups is dangling unco-ordinated (see Fig. 1). The co-ordination polyhedron can be described as a monocapped cube; bond distances and angles about the gadolinium atoms are listed in Table 2. The Gd–Cl distances vary between 2.675(6) and 2.737(6) Å, with a mean of 2.71(1) Å, and the Gd–N distances vary between 2.59(1) and 2.77(2) Å with a mean value of 2.68(2) Å. The mean values in related compounds[14] are 2.68(1) and 2.65(2) Å respectively. Carbon–carbon and –nitrogen distances have the expected values. The two halves of the bipyridyl groups are almost coplanar with torsion angles N(37)–C(36)–C(46)–N(47) 6(3) and N(37′)–C(36′)–C(46′)–N(47′) 2(2)°. The two cations are almost related by a glide plane at $y = 0$ and so have opposite chirality, a further difference is that the orientation of the non-co-ordinated pyridine groups differs by 180°. The pseudo-glide plane accounts for the ease with which zones of opposite polarity are achieved. The L^2 ligand forms six five-membered chelate rings with N–Gd–N angles in the range 59.1–61.7°. The mutual orientations of these chelate rings will in principle define the chirality of the molecule. However, the helical arrangement of the chain N(67), N(20), N(47), N(37), N(10), N(17) is a more

Table 2 Selected bond distances (Å) and angles (°) for $[\mathrm{GdL^2Cl_2}]\mathrm{Cl}\cdot 2\mathrm{H_2O}\cdot 0.5\mathrm{EtOH}$

Gd(1)–Cl(1)	2.712(6)	Gd(1′)–Cl(1′)	2.675(6)
Gd(1)–Cl(2)	2.724(5)	Gd(1′)–Cl(2′)	2.737(6)
Gd(1)–N(10)	2.770(21)	Gd(1′)–N(10′)	2.769(20)
Gd(1)–N(20)	2.651(18)	Gd(1′)–N(20′)	2.660(20)
Gd(1)–N(17)	2.770(10)	Gd(1′)–N(17′)	2.740(10)
Gd(1)–N(37)	2.586(11)	Gd(1′)–N(37′)	2.651(11)
Gd(1)–N(47)	2.606(10)	Gd(1′)–N(47′)	2.669(11)
Gd(1)–N(57)	2.661(10)	Gd(1′)–N(57′)	2.664(11)
Gd(1)–N(67)	2.652(11)	Gd(1′)–N(67′)	2.644(12)

Cl(1)–Gd(1)–Cl(2)	158.2(2)	Cl(1′)–Gd(1)–Cl(2′)	156.5(2)
Cl(1)–Gd(1)–N(10)	88.2(4)	Cl(1′)–Gd(1)–N(10′)	87.8(4)
Cl(1)–Gd(1)–N(20)	79.2(4)	Cl(1′)–Gd(1)–N(20′)	78.9(4)
Cl(1)–Gd(1)–N(17)	70.2(3)	Cl(1′)–Gd(1)–N(17′)	71.1(3)
Cl(1)–Gd(1)–N(37)	95.7(3)	Cl(1′)–Gd(1)–N(37′)	94.0(3)
Cl(1)–Gd(1)–N(47)	73.0(3)	Cl(1′)–Gd(1)–N(47′)	72.6(3)
Cl(1)–Gd(1)–N(57)	131.8(3)	Cl(1′)–Gd(1)–N(57′)	133.0(3)
Cl(1)–Gd(1)–N(67)	101.4(3)	Cl(1′)–Gd(1)–N(67′)	100.9(3)
Cl(2)–Gd(1)–N(10)	73.1(4)	Cl(2′)–Gd(1)–N(10′)	73.0(4)
Cl(2)–Gd(1)–N(20)	117.8(4)	Cl(2′)–Gd(1)–N(20′)	118.7(4)
Cl(2)–Gd(1)–N(17)	90.3(3)	Cl(2′)–Gd(1)–N(17′)	87.3(3)
Cl(2)–Gd(1)–N(37)	85.1(3)	Cl(2′)–Gd(1)–N(37′)	88.5(3)
Cl(2)–Gd(1)–N(47)	125.4(3)	Cl(2′)–Gd(1)–N(47′)	127.9(3)
Cl(2)–Gd(1)–N(57)	69.9(3)	Cl(2′)–Gd(1)–N(57′)	70.4(3)
Cl(2)–Gd(1)–N(67)	77.6(3)	Cl(2′)–Gd(1)–N(67′)	77.3(3)
N(10)–Gd(1)–N(20)	166.0(5)	N(10′)–Gd(1)–N(20′)	165.8(5)
N(10)–Gd(1)–N(17)	59.1(4)	N(10′)–Gd(1)–N(17′)	59.4(4)
N(10)–Gd(1)–N(37)	61.2(4)	N(10′)–Gd(1)–N(37′)	61.4(4)
N(10)–Gd(1)–N(47)	118.0(5)	N(10′)–Gd(1)–N(47′)	117.1(5)
N(10)–Gd(1)–N(57)	129.3(4)	N(10′)–Gd(1)–N(57′)	129.2(4)
N(10)–Gd(1)–N(67)	115.1(5)	N(10′)–Gd(1)–N(67′)	117.5(5)
N(20)–Gd(1)–N(17)	110.0(4)	N(20′)–Gd(1)–N(17′)	110.9(5)
N(20)–Gd(1)–N(37)	125.8(4)	N(20′)–Gd(1)–N(37′)	123.8(5)
N(20)–Gd(1)–N(47)	64.2(5)	N(20′)–Gd(1)–N(47′)	63.5(5)
N(20)–Gd(1)–N(57)	64.7(4)	N(20′)–Gd(1)–N(57′)	64.7(5)
N(20)–Gd(1)–N(67)	62.2(4)	N(20′)–Gd(1)–N(67′)	61.4(5)
N(17)–Gd(1)–N(37)	118.7(4)	N(17′)–Gd(1)–N(37′)	119.1(4)
N(17)–Gd(1)–N(47)	143.1(4)	N(17′)–Gd(1)–N(47′)	143.6(4)
N(17)–Gd(1)–N(57)	150.6(4)	N(17′)–Gd(1)–N(57′)	148.4(4)
N(17)–Gd(1)–N(67)	64.6(4)	N(17′)–Gd(1)–N(67′)	65.5(4)
N(37)–Gd(1)–N(47)	62.8(4)	N(37′)–Gd(1)–N(47′)	61.3(4)
N(37)–Gd(1)–N(57)	82.1(4)	N(37′)–Gd(1)–N(57′)	83.5(4)
N(37)–Gd(1)–N(67)	162.5(4)	N(37′)–Gd(1)–N(67′)	165.1(4)
N(47)–Gd(1)–N(57)	63.3(4)	N(47′)–Gd(1)–N(57′)	65.2(4)
N(47)–Gd(1)–N(67)	126.2(4)	N(47′)–Gd(1)–N(67′)	124.7(4)
N(57)–Gd(1)–N(67)	89.3(4)	N(57′)–Gd(1)–N(67′)	87.3(4)

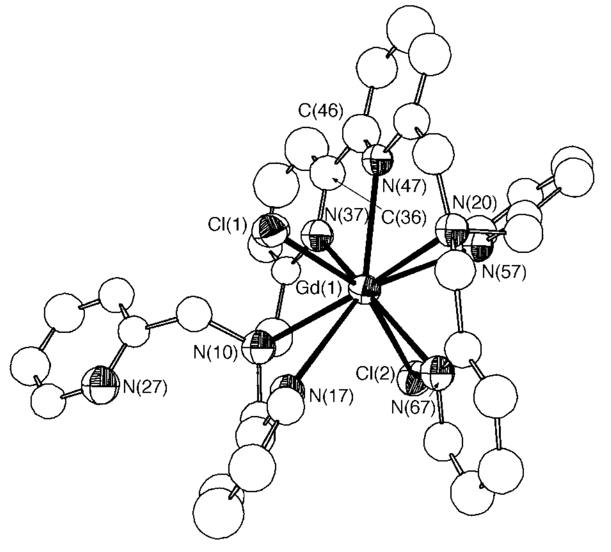

Fig. 1 View of one of the $[\mathrm{GdL^2\,Cl_2}]^+$ cations.[13] The thermal ellipsoids are drawn at the 50% probability level

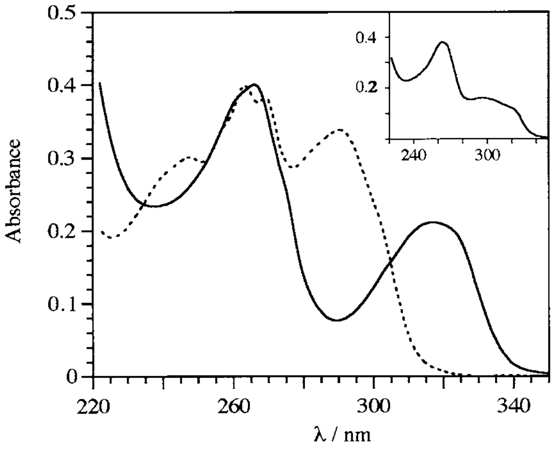

Fig. 2 Optical absorption spectra of complex **1** (——) and $\mathrm{L^2}$ (· · ·) in MeOH, $I = 0.1$ mol dm^{-3} $\mathrm{NBu_4ClO_4}$ both 2.00×10^{-5} mol dm^{-3} and of a 2.00×10^{-5} mol dm^{-3} aqueous solution of **1** (pH 7.0) at 296 K (inset). The cell length was 1.000 cm

obvious way to define the chirality in this case. This gives Δ for the complex cation in Fig. 1.

Optical absorption spectra

An absorption spectrum of $\mathrm{L^2}$ in MeOH is shown in Fig. 2. This consists of several bands, and the maxima at 246 and 288 nm are attributed to the bipyridine chromophore and those at 261 and 267 nm to the pyridine chromophores. Owing to low solubility, only a qualitative absorption spectrum of free $\mathrm{L^2}$ in water could be obtained,but it proved to be very similar to that taken in MeOH. The spectrum of **1** is very similar to that of free $\mathrm{L^2}$ in MeOH (Fig. 2), although a red shift is observed for the absorption band attributed to the bipyridine $\pi \longrightarrow \pi^*$ transition at 288 nm. The pyridine bands are, however, relatively unaffected by metal complexation. Complex **2** showed similar behaviour.

Concerning the stability of **1** in solution a spectrophotometric determination of the formation constant K_f [equation (1)] was carried out. By using MeOH, $I = 0.100$ mol dm^{-3}

$$\mathrm{M} + \mathrm{L} \xrightleftharpoons{K_\mathrm{f}} \mathrm{ML} \qquad (1)$$

$\mathrm{NBu_4ClO_4}$, as solvent instead of water the formation of hydroxo complexes and ligand protonation was avoided. The spectrum of solutions of **1** was measured over a wide range of concentrations. From the absorbance (A^{305}) at the isosbestic point at 305 nm the complex concentration could be calculated. The absorbance at 288 nm (A^{288}) can then be expressed as shown in equation (2).

$$A^{288} = \frac{l(\varepsilon_\mathrm{L}^{288} - \varepsilon_\mathrm{ML}^{288})}{2}\left(\sqrt{\frac{1}{K_\mathrm{f}^2} + \frac{4A^{305}}{l\varepsilon^{305}K_\mathrm{f}}} - \frac{1}{K_\mathrm{f}}\right) + \frac{\varepsilon_\mathrm{ML}^{288}}{\varepsilon^{305}}A^{305} \qquad (2)$$

In the derivation of equation (2) $\varepsilon_\mathrm{M}^{288}$ was neglected. Values for $\varepsilon_\mathrm{L}^{288}$ and ε^{305} were determined by independent experiments to be 16.9×10^3 and 7.70×10^3 dm^3 mol^{-1} cm^{-1}, respectively and the cell length, l, was 1.000 cm. The experimental values of A^{288} and A^{305} are plotted in Fig. 3. A least-squares fit refining $\varepsilon_\mathrm{ML}^{288}$ and K_f gave $K_\mathrm{f} = 10^{7.09 \pm 0.09}$ dm^3 mol^{-1} and $\varepsilon_\mathrm{ML}^{288} = 2.89(4) \times 10^3$ dm^3 mol^{-1} cm^{-1}. From the spectrum (Fig. 2, inset) of a 2.00×10^{-5} mol dm^{-3} solution of **1** in water the presence of free $\mathrm{L^2}$ is clearly seen. From the value of A^{288} (0.1546) a rough estimate of K_f in water (pH 7.0) can be obtained assuming that the values of $\varepsilon_\mathrm{L}^{288}$ and $\varepsilon_\mathrm{ML}^{288}$ in water are similar to the values in MeOH. This gives $K_\mathrm{f} \approx 10^{5.4}$ dm^3 mol^{-1} showing that the $\mathrm{H_2O}$ ligands are more strongly bound to the metal than are the MeOH ligands. From aqueous solutions of **1** precipitation of free $\mathrm{L^2}$ was observed at complex concentrations above $\approx 5 \times 10^{-5}$ mol dm^{-3}.

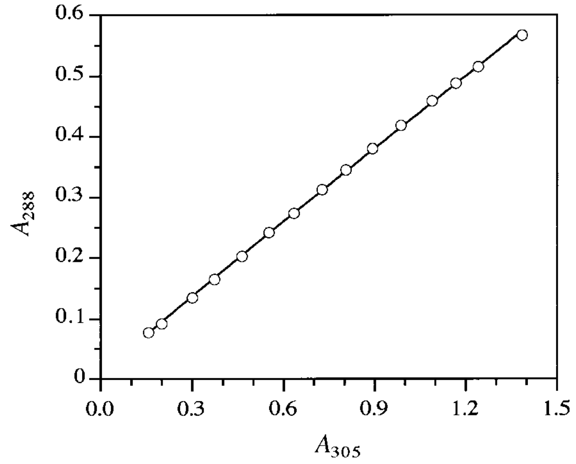

Fig. 3 Absorbance at 288 nm *vs.* absorbance at 305 nm of methanol, $I = 0.100$ mol dm^{-3} NBu_4ClO_4, solutions of $[EuL^2]Cl_3{\cdot}1.5H_2O$. Circles represent experimental data and the line a least-squares fit using equation (2)

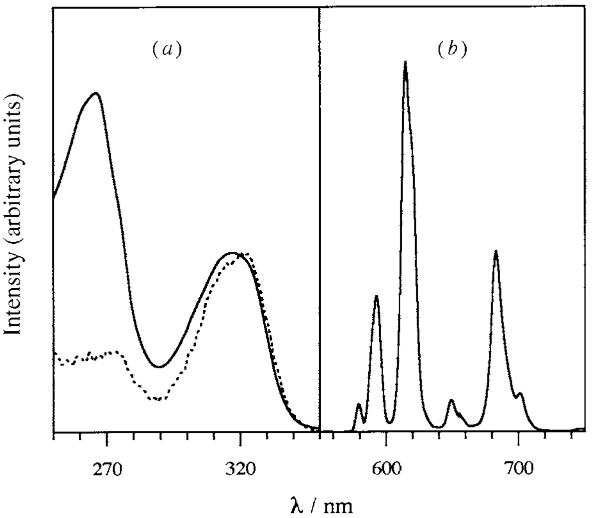

Fig. 4 (*a*) Excitation spectrum (----, $\lambda_{em} = 613$ nm) of complex **1** in water at 296 K. For comparison the absorption spectrum (——) of **1** in MeOH is shown. (*b*) Emission spectrum ($\lambda_{ex} = 320$ nm) of **1** in water at 296 K

Luminescence

Complex **1** is highly luminescent in the solid state and in water and MeOH solutions. The room-temperature luminescence spectrum of **1** in water is shown in Fig. 4(*b*). The spectrum, which is similar to that of **1** in MeOH, displays strong, sharp peaks which have been assigned as the $^5D_0 \longrightarrow {}^7F_J$ transitions, the peaks at various *J* levels (0–6) of the ^7F_J manifold.[15] The emission spectra of **1** in D_2O and CH_3OD were identical to that recorded in aqueous solution. In frozen aqueous or MeOH solution at 77 K the emission decreased in intensity and showed only a broad featureless luminescence centred at around 640 nm. Upon thawing, the emission spectra and lifetimes recover completely. We have no simple explanation for these observations. The quantum yields for luminescence of the most intense band ($\lambda = 613$ nm, assigned to the $^5D_0 \longrightarrow {}^7F_2$ transition) in water and D_2O at 296 K were found to be 0.022 ± 0.003 and 0.041 ± 0.003, respectively. The integrated intensity of all the $^5D_0 \longrightarrow {}^7F_2$ transitions gives the respective quantum yields of 0.046 and 0.089. The emission lifetimes determined at 613 nm for solid **1** and for water, D_2O, MeOH and CH_3OD solutions of **1** are listed in Table 3. The presence of Eu^{3+}(aq), the product of ligand dissociation from the EuL^2 complex, does not interfere with the measurements since it is virtually non-luminescent under these conditions (luminescence is quenched by the H_2O ligands). Neither does the presence of free L^2 interfere with the quantum-yield measurements since it does not absorb at the excitation wavelength (320 nm, see Fig. 2). Thus, only rigorously unexponential decays were observed. The average number of H_2O ligands (n_{H_2O}) co-ordinated to the $[EuL^2]^{3+}$ emitter in aqueous solution can be estimated according to the empirical correlation (3) proposed by Horrocks.[17a,b]

Table 3 Metal luminescence lifetimes ($\lambda_{ex} = 355$ nm) in water, D_2O, MeOH and MeOD at 296 K and in the solid state at 77 and 296 K

	$[EuL^2]Cl_3{\cdot}1.5H_2O$	$[EuL^1]Cl_3{\cdot}6H_2O$
$\tau^{296}_{H_2O}$/ms	0.780	0.34^a
$\tau^{296}_{D_2O}$/ms	1.28	1.70^a
τ^{296}_{MeOH}/ms	0.980	*b*
τ^{296}_{MeOD}/ms	1.25	*b*
τ^{296}_{solid}/ms	0.80	0.95^c
τ^{77}_{solid}/ms	1.15	*b*

[a] Ref. 1(*b*). [b] Not reported. [c] At 300 K, ref. 16.

$$n_{H_2O} = k[(1/\tau^{296}_{H_2O}) - (1/\tau^{296}_{D_2O})] \qquad (3)$$

Here $\tau^{296}_{H_2O}$ and $\tau^{296}_{D_2O}$ denote the emission lifetime at 296 K in water and D_2O solution, respectively, *k* is a constant, 1.05, empirically determined for Eu^{III} and the value of n_{H_2O} is considered to have an uncertainty of ±0.5. Use of equation (3) with the lifetimes listed in Table 3 gave $n_{H_2O} = 0.5$. The number of co-ordinated MeOH molecules in MeOH solution can be calculated analogously by using the lifetimes determined in MeOH and MeOD.[17c] In this case the number of OH oscillators in a co-ordinated MeOH molecule is half that of a co-ordinated H_2O, thus a different *k* is used (2.1). In this manner it was shown that n_{MeOH} also equals 0.5. However, the structure of the GdL^2 complex predicts n_{MeOH} and $n_{H_2O} = 2$ (after substitution of the chloride ligands). One possible explanation for this discrepancy is the occurrence of structural changes on going from the solid state to a solution, where the unco-ordinated pyridine group present in the solid state is co-ordinated to the metal in solutions (water or MeOH) of complexes Eu^{III} and Gd^{III} of L^2. Comparison of the excitation spectrum and absorption spectrum of **1** [Fig. 4(*a*)] reveals that the relative intensity of the pyridine-centred absorption (265 nm) compared with the bipyridine-centred absorption (320 nm) is much lower than in the absorption spectrum. Thus, the energy transfer from the pyridine groups to the metal is apparently inefficient.

In summary, the complex $[EuL^2]Cl_3{\cdot}1.5H_2O$ is luminescent in the solid state and in MeOH and water solutions. In both solvents the average number of solvent molecules co-ordinated to the metal is 0.5. Compared to the EuL^1 system[1a] the present study shows that the more flexible L^2 ligand more efficiently wraps the metal ion and thereby serves to shield it much more effectively from solvent molecules. Another more complicated ligand with four bipy moieties, two within a hexaazamacrocycle and two in pendant groups, is somewhat better in excluding water from the europium(III) co-ordination sphere, but is also somewhat unstable.[1f] Major drawbacks in the EuL^2 system are the instability to dissociation in water and the poor antenna properties of the pyridine groups, which results in smaller efficiency in converting incident ultraviolet photons into emitted visible photons.

Acknowledgements

P. C. F. is indebted to support by the U.S. National Science Foundation (Grant No. CHE-9400919). Laser flash photolysis experiments were carried out on a time-resolved optical system constructed using partial support from a US Department of Energy University Research Instrumentation Grant (No. DE-FG05-91ER79039) and in part from a National Science Foundation Instrumentation Grant. A. D. is indebted to the Danish Natural Science Research Council (Grant No. 11-5962) for the UV/VIS spectrophotometer. A. H. is indebted to the Carlsberg Foundation and to the Danish Natural Science Research Council for the diffractometer.

References

1 (*a*) B. Alpha, J.-M. Lehn and G. Mathis, *Angew. Chem., Int. Ed. Engl.*, 1987, **26**, 266; (*b*) B. Alpha, R. Ballardini, V. Balzani, J.-M. Lehn, S. Perathoner and N. Sabbatini, *Photochem. Photobiol.*, 1990, **52**, 299; (*c*) L. Prodi, M. Maestri, R. Ziessel and V. Balzani, *Inorg. Chem.*, 1991, **30**, 3798; (*d*) N. Sabbatini, M. Guardigli, I. Manet and F. Bolletta, *Inorg. Chem.*, 1994, **33**, 955; (*e*) V. Balzani, E. Berghmans, J.-M. Lehn, N. Sabbatini, R. Terörde and R. Ziessel, *Helv. Chim. Acta*, 1990, **73**, 2083; (*f*) V. Balzani, J.-M. Lehn, N. Sabbatini and R. Ziessel, *Angew. Chem., Int. Ed. Engl.*, 1991, **30**, 190; (*g*) J. Bruno, B. R. Herr and W. DeW. Horrocks, jun., *Inorg. Chem.*, 1993, **32**, 756; (*h*) G. Bernardinelli, C. G. Bochet, J.-C. G. Bünzli, P. Froidevaux and C. Piguet, *J. Chem. Soc., Dalton Trans.*, 1995, 83.

2 V. Balzani and F. Scandola, *Supramolecular Photochemistry*, Eltis Horwood, Chichester, 1991.

3 I. Bkouche-Waksman, J. Guilhem, C. Pascard, B. Alpha, R. Deschenaux and J.-M. Lehn, *Helv. Chim. Acta*, 1991, **74**, 1163.

4 A. Døssing, A. Hazell and H. Toftlund, *Acta Chem. Scand.*, 1996, **50**, 95.

5 S. Parkin, B. Moezzi and H. Hope, *J. Appl. Crystallogr.*, 1995, **28**, 53.

6 A. Altomare, G. Cascarano, C. Giacovazzo, A. Guagliard, M. C. Burla, G. Polidori and M. Camalli, *J. Appl. Crystallogr.*, 1994, **27**, 435.

7 R. G. Hazell, LINKON, a Program for Constrained Least-squares Refinement, Aarhus University, Århus, 1995.

8 D. Rogers, *Acta Crystallogr., Sect. A*, 1981, **37**, 734.

9 *International Tables for X-Ray Crystallography*, Kynoch Press, Birmingham, 1974, vol. 4, pp. 72–98.

10 K. R. Kyle, C. K. Ryu, J. A. DiBenedetto and P. C. Ford, *J. Am. Chem. Soc.*, 1991, **113**, 2954; M. M. Mdleleni, J. S. Bridgewater, R. J. Watts and P. C. Ford, *Inorg. Chem.*, 1995, **34**, 2334.

11 J. van Houton and R. J. Watts, *J. Am. Chem. Soc.*, 1976, **98**, 4853.

12 Y. Haas and G. Stein, *J. Phys. Chem.*, 1971, **75**, 3668.

13 C. K. Johnson, ORTEP II, Report ORNL-5138, Oak Ridge National Laboratory, Oak Ridge, TN, 1976.

14 F. H. Allen, J. E. Davies, J. J. Galloy, O. Johnson, O. Kennard, C. F. Macrae, E. M. Michell, G. F. Michell, J. M. Smith and D. G. Watson, *J. Chem. Inf. Comput. Sci.*, 1991, **31**, 187.

15 J.-C. G. Bünzli, *Lanthanide Probes in Life, Chemical and Earth Sciences*, Elsevier, Amsterdam, 1989, ch. 7.

16 G. Blasse, G. J. Dirksen, D. van der Voort, N. Sabbatini, S. Perathoner, J.-M. Lehn and B. Alpha, *Chem. Phys. Lett.*, 1988, **146**, 346.

17 (*a*) W. DeW. Horrocks, jun. and D. R. Sudnick, *J. Am. Chem. Soc.*, 1979, **101**, 334; (*b*) W. DeW. Horrocks, jun. and D. R. Sudnick, *Acc. Chem. Res.*, 1981, **14**, 384; (*c*) W. DeW. Horrocks, jun., *Inorg. Chem.*, 1991, **30**, 3270.

Received 13*th May* 1996; *Paper* 6/03336I